

Learning Discriminative Features with Multiple Granularities for Person Re-Identification

Guanshuo Wang^{1*}, Yufeng Yuan^{2*}, Xiong Chen², Jiwei Li², Xi Zhou^{1,2}

¹ Cooperative Medianet Innovation Center, Shanghai Jiao Tong University

² CloudWalk Technology Co., Ltd.

guanshuo.wang@sjtu.edu.cn

{yuanyufeng, chenxiong, lijawei, zhoxi}@cloudwalk.cn

Abstract

The combination of global and partial features has been an essential solution to improve discriminative performances in person re-identification (Re-ID) tasks. Previous part-based methods mainly focus on locating regions with specific pre-defined semantics to learn local representations, which increases learning difficulty but not efficient or robust to scenarios with large variances. In this paper, we propose an end-to-end feature learning strategy integrating discriminative information with various granularities. We carefully design the Multiple Granularity Network (MGN), a multi-branch deep network architecture consisting of one branch for global feature representations and two branches for local feature representations. Instead of learning on semantic regions, we uniformly partition the images into several stripes, and vary the number of parts in different local branches to obtain local feature representations with multiple granularities. Comprehensive experiments implemented on the mainstream evaluation datasets including Market-1501, DukeMTMC-reid and CUHK03 indicate that our method has robustly achieved state-of-the-art performances and outperformed any existing approaches by a large margin. For example, on Market-1501 dataset in single query mode, we achieve a state-of-the-art result of Rank-1/mAP=96.6%/94.2% after re-ranking.

1. Introduction

Person re-identification (Re-ID) is a challenging task to retrieve a given person among all the gallery pedestrian images captured across different security cameras. Due to the scene complexity of images from surveillance videos, the main challenges for person Re-ID come from large variations on persons such as pose, occlusion, clothes, background clutter, detection failure, etc. The blossom of deep

*Equal contribution



Figure 1. Body part partition from coarse to fine granularities. We regard original pedestrian images with the whole body as the coarsest level of granularity in the left column. The middle and right column are respectively pedestrian partitions divided into 2 and 3 stripes from the original images. The more stripes images are divided into, the finer the granularity of partitions is.

convolutional network has introduced more powerful representations with better discrimination and robustness for pedestrian images, which pushed the performance of Re-ID to a new incredible level. Just during recent months, some deep Re-ID methods [3, 40, 34, 26] have achieved breakthrough with high-level identification rates and mean average precision.

The intuitive approach of pedestrian representations is to extract discriminative features from the whole body on images. The aim of global feature learning is to capture the most salient information among all the different persons, e.g. colors of clothes, to represent identities of pedestrians. However, high complexity for images captured in surveillance scenes usually restrict the accuracy for feature learning in large scale Re-ID scenarios. For the limited scale and weak diversity of person Re-ID training datasets, some non-salient or infrequent detailed information can be easily ignored and make no contribution for better discrimina-

tion during global feature learning procedure, which makes global features hard to adapt conditions of similar inter common properties or large intra variances.

To relieve this dilemma, locating significant body parts from images to represent local information for identities has been discovered as an effective approach for better Re-ID accuracy in many previous works. Each located body part region only contains a small percentage of local information from the whole body, and at the same time distraction by other related or unrelated information outside the regions is actually filtered by locating operations, with which local features can be learned to concentrate more on identities and used as an important complement for global features. Part-based methods for person Re-ID can be divided into three main pathways according to their part locating methods: 1) locating partial regions with strong structural information such as empirical knowledge about human bodies [34, 40] or strong learning-based pose estimation [32, 42]. 2) locating partial regions with region proposal methods [38, 19]. 3) Enhancing features by middle-level attention on salient parts [43, 25, 24, 22]. However, obvious limitations impede the effectiveness of these methods. First, pose or occlusion variations can affect the reliability of local representation. Second, these methods almost only focus on specific parts with fixed semantics, but cannot cover all the discriminative parts. Last but not least, most of these methods are not end-to-end learning process, which increases the difficulty of learning.

In this paper, we propose a feature learning strategy combining global and local information in different granularities. As shown in Figure 1, various numbers of partition stripes introduce a diversity of granularity: we define Global Branch containing only one whole partition with global information as the coarsest case. As the number of partitions increase, features of local parts can concentrate more on finer discriminative information in each part stripe, with filtering information on the other stripes. Since deep learning mechanism can capture approximate attention on the main body from the whole image, it is also possible to capture more concentrated saliency preferences for local features extracted from different partial regions. Based on this idea, we design the Multiple Granularity Network (MGN), a multi-branch network architecture divided into one global and two local branches with delicated parameters from the 4th residual stage of the ResNet-50 [14] backbone. In each local branch of MGN, we divide globally-pooled feature maps into different numbers of stripes as part regions to learn local feature representations independently, referring the methods in [40, 34]. Comparing to the previous part-based methods, our method only utilize equally-divided parts for local representation, but can achieve outstanding performance exceeding all previous methods. Extensive experiment results show that

our method can achieve state-of-the-art performances on several mainstream Re-ID datasets without any additional external data or re-ranking [49] operation. Besides, our method is completely end-to-end learning process, which is easy for learning and implementation. We observe that the multi-branch architecture of MGN cooperatively boosts the representation performance of any single branch comparing to the same single branch settings.

2. Related Work

The blossom of deep learning also drove the development of Re-ID systems. [20, 39] first introduce deep siamese network architecture into Re-ID and combine the body part features, achieving higher performance comparing to the contemporary hand-crafted methods. [45] proposes ID-discriminative Embedding (IDE) with simple ResNet-50 backbones as a baseline of the performance level for modern deep Re-ID systems. In [1, 35], mid-level features of image pairs are computed to depict interrelation of local parts with carefully designed mechanism. [37] introduces Domain Guided Dropout to enhance the generalization ability across different domains of pedestrian scenarios. [8] combines global and local features from multi-channels and learns discriminative representations with improved triplet loss function. [24, 25, 38, 43, 19, 22] utilize attention information within the embedding to improve the representing discrimination on local parts of bodies. [42, 32] use structural information of body landmarks for accurate semantic local part region proposals.

In recent months, some deep Re-ID methods pushed the performances to a new level comparing to the former systems. [40] introduces a part-based alignment matching in training phase with shortest path programming and mutual learning to improve metric learning performance. [3, 34] both equally slice the feature maps of input images into several stripes in vertical orientation. [3] merges slices of part features with LSTM network and combine with global features learned from classification metric learning. Instead [34] directly concatenates the features from local parts as the final representation, and applies refined part pooling to modify the mapping validation of part features. However, according to the view in [40], these systems just achieve similar performances as human. Our proposed method

3. Multiple Granularity Network

3.1. Network Architecture

The architecture of Multiple Granularity Network is shown in Figure 2. The backbone of our network is ResNet-50 [14] which helps to achieve competitive performances in some Re-ID systems [40, 3, 34]. The most obvious modification different from the original version is that we divide the subsequent part after *res_conv4_1* block into three inde-

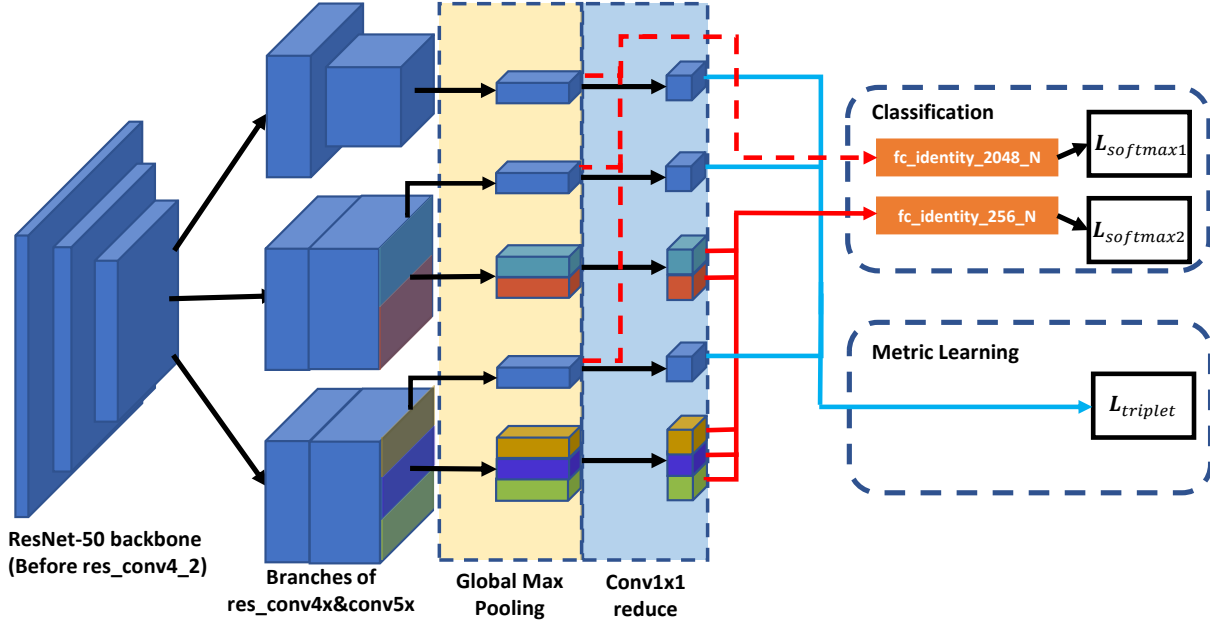


Figure 2. Multiple Granularity Network architecture. The ResNet-50 backbone is split into three branches after res_conv4_1 residual block: Global Branch, Part-2 Branch and Part-3 Branch. During testing, all the reduced features are concatenated together as the final feature representation of a pedestrian image. Notice that the 1×1 convolutions for dimension reduction and fully connected layers for identity prediction in each branch **DO NOT** share weights with each other. Each path from the feature to the specific loss function represents an independent supervisory signal.

pendent branches, sharing the similar architecture with the original ResNet-50.

Table 1 compares the settings of these branches. In the upper branch, we employ down-sampling with a stride-2 convolution layer in res_conv5_1 block, following a global max-pooling (GMP) operation on the corresponding output feature map and a 1×1 convolution layer with batch normalization [17] and ReLU to reduce 2048-dim features \mathbf{z}_g^G to 256-dim \mathbf{f}_g^G . This branch learns the global feature representations without any partition information, so we name this branch as the **Global Branch**.

The middle and lower branches both share the similar network architecture with Global Branch. The difference is that we employ no down-sampling operations in res_conv5_1 block, and output feature maps in each branch are uniformly split into several stripes in horizontal orientation, on which we independently perform the same following operations as Global Branch to learn local feature representations. We call these branches **Part- N Branch**, where N refers to the number of partitions on the unreduced feature maps, e.g. the middle and lower branches in Figure 2 can be named as Part-2 and Part-3 Branch.

During testing phases, to obtain the most powerful discrimination, reduced features are concatenated as the final feature, which combines both the global and local information to perfect the comprehensiveness for learned features.

Branch	Part No.	Map Size	Dims	Feature
Global	1	12×4	256	\mathbf{f}_g^G
Part-2	2	24×8	$256 \times 2 + 256$	$\{\mathbf{f}_{p_i}^{P2} _{i=1}^2\}, \mathbf{f}_g^{P2}$
Part-3	3	24×8	$256 \times 3 + 256$	$\{\mathbf{f}_{p_i}^{P3} _{i=1}^3\}, \mathbf{f}_g^{P3}$

Table 1. Comparison of the settings for three branches in MGN. Here the size of input images is set to 384×128 .

3.2. Loss Functions

To unleash the discrimination ability of the learned representations of this network architecture, we employ softmax loss for classification, and triplet loss for metric learning as the loss functions in training phases, which are both widely used in various deep Re-ID methods.

For basic discrimination learning, we regard the identification task as a multi-class classification problem. For i -th learned features \mathbf{f}_i , softmax loss is formulated as:

$$L_{softmax} = - \sum_{i=1}^N \log \frac{e^{\mathbf{W}_{y_i}^T \mathbf{f}_i + b_{y_i}}}{\sum_{k=1}^C e^{\mathbf{W}_k^T \mathbf{f}_i + b_k}} \quad (1)$$

where N is the size of mini-batch in training process and C is the number of classes in the training dataset. Among all the learned embeddings, we employ the softmax loss to the global features before 1×1 convolution reduction $\{\mathbf{z}_g^G, \mathbf{z}_g^{P2}, \mathbf{z}_g^{P3}\}$ and part features after reduction $\{\mathbf{f}_{p_i}^{P2} |_{i=1}^2, \mathbf{f}_{p_i}^{P3} |_{i=1}^3\}$.

All the global features after reduction $\{\mathbf{f}_g^G, \mathbf{f}_g^{P2}, \mathbf{f}_g^{P3}\}$ are trained with triplet loss to enhance ranking performances. We use the batch-hard triplet loss [15], an improved version based on the original semi-hard triplet loss. This loss function is formulated as follows:

$$L_{triplet} = - \sum_{i=1}^P \sum_{a=1}^K [\alpha + \max_{p=1\dots K} \|\mathbf{f}_a^{(i)} - \mathbf{f}_p^{(i)}\|_2 - \min_{\substack{n=1\dots K \\ j=1\dots P \\ j \neq i}} \|\mathbf{f}_a^{(i)} - \mathbf{f}_n^{(j)}\|_2]_+ \quad (2)$$

where $\mathbf{f}_a^{(i)}, \mathbf{f}_p^{(i)}, \mathbf{f}_n^{(i)}$ are the features extracted from anchor, positive and negative samples respectively. Here positive and negative samples refer to the pedestrians with same or different identity with the anchor. The candidate triplets are built by the furthest positive and closest negative sampled pairs, *i.e.* the hardest positive and negative pairs in a mini-batch with P selected identities and K images from each identity. This improved version of triplet loss enhances the robustness in metric learning, and further improve the performances at the same time.

3.3. Discussions

Multi-branch architecture According to our initial motivation for MGN architecture, it seems to be reasonable that the global and local representations are both learned in one single branch. We can directly split the same final feature maps in different numbers of stripes, and apply corresponding supervisory signals as our proposed methods. However, we find this setting is not efficient for further performance improving. We speculate the branches sharing the similar network architecture (mainly the fourth residual stage of ResNet-50) just response to the detailed information on images. Learning features in multiple granularities but mixed to one whole network might dilute the importance of detailed information. Besides, we try to split the backbone network after shallower or deeper layers, which also achieve no better performances.

Diversity of granularity Three branches in our network architecture actually learn representing information with different emphasis. Global Branch with larger reception field and global max-pooling captures integral but coarse features from the pedestrian images, and features learned by Part-2 and Part-3 Branches without strided convolution and split parts of stripes tend to be local but fine. The branch with more split parts will learn finer representation for pedestrian images. Branches learning different preferences can cooperatively supplement low-level discriminating information to the common backbone parts, which might be the reason for performance boosting in any single branch.

4. Experiment

4.1. Implementation

To capture more detailed information from pedestrian images, we refer to [34] and resize input images to 384×128 . We use the weights of ResNet-50 pretrained on ImageNet [9] to initialize the backbone and branches of MGN. Notice that different branches in the network are all duplicated with the pretrained weights of the corresponding layers after the block *res_conv4.1*. During training phases, we only deploy random horizontal flipping to images in training sets for data augmentation. Each mini-batch is sampled with randomly selected P identities and randomly sampled K images for each identity from the training set to cooperate the requirement of triplet loss. Here we recommend to set $P = 16$ and $K = 4$ to train our proposed model. We choose SGD as the optimizer with momentum 0.9. The weight decay factor for L2 regularization is set to 0.0005. As for the learning rate strategy, we set the initial learning rate to 0.01, and decay the learning rate to $1e-3$ and $1e-4$ after training for 40 and 60 epochs. The total training process lasts for 80 epochs. During evaluation, we both extract the features corresponding to original images and the horizontally flipped versions, then use the average of these as the final features. Our model is implemented on PyTorch framework. To conduct a complete training procedure on Market-1501 dataset, it takes about 2 hours with data-parallel acceleration by two NVIDIA TITAN Xp GPUs. All our experiments on different datasets follow the settings above.

4.2. Datasets and Protocols

The experiments to evaluate our proposed method are conducted on three mainstream Re-ID datasets: Market-1501 [44], DukeMTMC-reID [48] and CUHK03 [20]. It is necessary to introduce these datasets and their evaluation protocols before we show our results.

Market-1501 This dataset includes images of 1,501 persons captured from 6 different cameras. The pedestrians are cropped with bounding-boxes predicted by DPM detector [11]. The whole dataset is divided into training set with 12,936 images of 751 persons and testing set with 3,368 query images and 19,732 gallery images of 750 persons. There are single-query and multiple-query modes in evaluation, the difference of which is the number of images from the same identity. In multiple-query mode, all features extracted from the images of a person captured by the same camera are merged by avg- or max-pooling, which contains more complete information than single query mode with only 1 query image.

DukeMTMC-reID This dataset is a subset of the DukeMTMC [27] used for person re-identification by images. It consists of 36,411 images of 1,812 persons from 8 high-resolution cameras. 16,522 images of 702 persons are

randomly selected from the dataset as the training set, and the remaining 702 persons are divided into the testing set where contains 2,228 query images and 17,661 gallery images. It might be the most challenging datasets for person Re-ID at present, with common situations in high similarity across persons and large variations within the same identity.

CUHK03 This dataset consists of 14,097 images of 1,467 persons from 6 cameras. Two types of annotations are provided in this dataset: manually labeled pedestrian bounding boxes and DPM-detected bounding boxes. Originally the whole dataset is divided into 20 random splits for cross-validation, which is designed for hand-crafted methods and very time-consuming to conduct experiments for deep-learning-based methods.

Protocols In our experiments, to evaluate the performances of Re-ID methods, we report the cumulative matching characteristics (CMC) at rank-1, rank-5 and rank-10, and mean average precision (mAP) on all the candidate datasets. On Market-1501 dataset, we conduct experiments both in single-query and multiple-query mode. On CUHK03 dataset, to simplify the evaluation procedure and meanwhile enhance the accuracy of the performance reflected by the results, we adopt the protocol used in [49].

4.3. Effectiveness of Components

To verify effectiveness of each component in MGN, we conduct several ablation experiments with different component settings on Market-1501 dataset in single query mode. Notice that other unrelated settings in each comparative experiment are the same as MGN implementation in Section 4.1, and we have carefully tuned all the candidate models and report the best performance with our settings. Table 2 shows the comparison results in different settings related to components of MGN. We separately analyze each component as follows:

MGN vs ResNet-50 Comparing the results by the baseline ResNet-50 model with our MGN model without triplet loss, we can observe MGN makes a significant performance improvement from Rank-1/mAP=87.5%/71.4% to 95.3%/86.2% (+7.8%/14.8%). We also implement the same experiment with ResNet-101 model, which has a similar scale of weights with MGN. The deeper ResNet-101 network indeed brings a considerable performance boost (+2.9%/7.4%), but there is still a large gap with our MGN model, which shows that extra weights from additional branches are not the main contributors of the improvement, but the carefully-designed network architecture. Results above prove that our proposed MGN has incredible capability of feature representations for person Re-ID.

Triplet Loss A number of previous works [20, 8, 40, 3] have shown the effectiveness of joint training with softmax loss for classification and triplet loss for metric learning in person Re-ID tasks. In our experiments, we reproduce

Model	Rank-1	Rank-5	Rank-10	mAP
ResNet-50	87.5	94.9	96.7	71.4
ResNet-101	90.4	95.7	97.2	78.0
ResNet-50+TP	88.7	96.0	97.2	75.0
Global (Branch)	89.8	95.8	97.5	78.5
Part-2 (Single)	92.6	97.1	98.0	80.2
Part-2 (Branch)	94.4	97.9	98.8	83.9
Part-3 (Single)	93.1	97.6	98.7	82.1
Part-3 (Branch)	94.4	98.2	98.8	84.1
G+P2+P3 (Single)	94.4	97.6	98.5	85.2
MGN w/o TP	95.3	97.9	98.7	86.2
MGN	95.7	98.3	99.0	86.9

Table 2. Results with different settings on Market-1501 datasets. "TP" refers to triplet loss. "Branch" refers to a sub-branch of MGN. "Single" refers to a single network with the same setting as the branch with the corresponding name in MGN. The model "ResNet-50+TP" can be regarded as "Global (Single)". "G+P2+P3" refers to an ensemble setting by Global (Single), Part-2 (Single) and Part-3 (Branch).

the boosting effect with both ResNet-50 and MGN models. With the help of triplet loss on all the candidate datasets, we can observe +1.2%/3.6% Rank-1/mAP improvement to the baseline model, and +0.4%/0.7% Rank-1/mAP improvement to MGN model. We can obvious two interesting effects from the improvement figures: 1) The improvement on mAP is more obvious than that on rank-1 accuracy, which proves the ranking effects of metric learning losses. 2) Triplet loss brings larger improvement to the baseline model than that to MGN. Comparing to softmax loss, triplet loss helps to capture more detailed information to meet the margin condition [29]. Our proposed network architecture is initially designed to enhance the local representation, which dilutes the original effects of triplet loss.

Multi-branch architecture The multi-branch setting in one single network is very similar to ensemble of multiple independent networks, but we believe the cooperation of multiple branches can achieve a better performance than ensemble learning. We train three independent ResNet-50 networks separately, each of which respectively replicates the corresponding configuration of three branches, *i.e.* Global, Part-2 and Part-3 Branch in MGN. In our experiments, we explore the effects of multi-branch architecture in two aspects. On the one hand, from a global view, we compare the performance of MGN with the ensemble of three single networks. The ensemble strategy indeed achieves better performance than any single participating network, but MGN still outperforms about 1% ~ 2% on both Rank-1 and mAP. It shows that the cooperation of branches learns more discriminative feature representations than independent networks. On the other hand, from a local view, we respectively compare the performances of features learned by sub-branches

Methods	Single Query		Multiple Query	
	Rank-1	mAP	Rank-1	mAP
MSCAN[19]	80.3	57.5	86.8	66.7
DLPA[43]	81.0	63.4	-	-
SVDNet[33]	82.3	62.1	-	-
PDC[32]	84.1	63.4	-	-
TriNet[15]	84.9	69.1	90.5	76.4
JLML[21]	85.1	65.5	89.7	74.5
DML[41]	87.7	68.8	91.7	77.1
DPFL[7]	88.6	72.6	92.2	80.4
HA-CNN[22]	91.2	75.7	93.8	82.8
GP-reid[2]	92.2	81.2	94.7	87.3
PCB [34]	92.3	77.4	-	-
Deep-Person[3]	92.3	79.6	94.5	85.1
Aligned-ReID[40]	92.6	82.3	-	-
PCB+RPP[34]	93.8	81.6	-	-
MGN(Ours)	95.7	86.9	96.9	90.7
TriNet(RK)[15]	86.7	81.1	91.8	87.2
GP-reid(RK)[2]	92.2	90.0	94.2	91.2
Aligned-ReID(RK)[40]	94.0	91.2	-	-
MGN(Ours, RK)	96.6	94.2	97.1	95.9

Table 3. Comparison of results on Market-1501 with Single Query setting (SQ) and Multiple Query setting (MQ). "RK" refers to implementing re-ranking operation.

of MGN with single networks in corresponding setting of branch. As our expect, the features from sub-branches also perform better than that from single networks. We argue that the mutual effects between sub-branches complement the blind spots in their individual learning procedure.

4.4. Comparison with State-of-the-Art Methods

We compare our proposed method with current state-of-the-art methods on all the candidate datasets to show our considerable performance advantage over all the existing competitors. Results in detail are given as follow:

Market-1501 The results on Market-1501 dataset is shown in Table 3. For the special effects of re-ranking method for improvement on mAP and rank-1 accuracy, we divide the results into two groups according to whether re-ranking is implemented or not. Among the results by other methods without re-ranking in single query mode, PCB+RPP [34] achieved the best published result, but our MGN achieves Rank-1/mAP=95.7%/86.9%, exceeding the former method by 1.9% in Rank-1 accuracy and 5.3% in mAP. After implementing re-ranking, the result can be improved to Rank-1/mAP=96.6%/94.2%, which surpasses all existing methods by a large margin.

DukeMTMC-reID According to Table 4, our MGN architecture also performs excellently on the challenging DukeMTMC-reID dataset. GP-reid [2] is a good practice of many useful strategies combined in person Re-ID tasks and achieved the best published result. MGN achieves state-of-

Methods	Rank-1	mAP
PAN[47]	71.6	51.5
FMN[10]	74.5	56.9
SVDNet[33]	76.7	56.8
PSE[28]	79.8	62.0
HA-CNN[22]	80.5	63.8
Deep-Person[3]	80.9	64.8
PCB[34]	83.3	69.2
GP-reid[2]	85.2	72.8
MGN(Ours)	88.7	78.4

Table 4. Comparison of results on DukeMTMC-reID.

Methods	Labeled		Detected	
	Rank-1	mAP	Rank-1	mAP
BOW+XQDA[44]	7.9	7.3	6.4	6.4
LOMO+XQDA[23]	14.8	13.6	12.8	11.5
IDE[45]	22.2	21.0	21.3	19.7
PAN[47]	36.9	35.0	36.3	34.0
SVDNet[33]	40.9	37.8	41.5	37.3
HA-CNN[22]	44.4	41.0	41.7	38.6
MLFN[4]	54.7	49.2	52.8	47.8
PCB[34]	-	-	61.3	54.2
PCB+RPP[34]	-	-	63.7	57.5
MGN(Ours)	68.0	67.4	66.8	66.0

Table 5. Comparison of results on CUHK03 with evaluation protocols in [49].

the-art result of Rank-1/mAP=88.7%/78.4%, outperforming GP-reid by +3.5% in Rank-1 and +5.6% in mAP. Standing on this level of performance on the most challenging datasets currently, we believe there are still some issues to be conquered for further perfect deep Re-ID systems.

CUHK03 As shown in Table 5, MGN achieves Rank-1/mAP=68.0%/67.4% on CUHK03 labeled setting and 66.8%/66.0% on CUHK03 detected setting, which outperforms to all the published results by a large margin. Here we can observe an obvious gap between results of labeled and detected conditions. We argue that it reflects an important affect of detection failure on person Re-ID performance, which emphasizes the importance of high-performance pedestrian detectors.

5. Conclusion

In this paper, we propose the Multiple Granularity Network (MGN), a novel multi-branch deep network for learning discriminative representations in person re-identification tasks. Each branch in MGN learns global or local representation with certain granularity of body partition. Our method directly learns local features on horizontally-split feature stripes, which is completely end-

to-end and introduces no part locating operations such as region proposal or pose estimation. Extensive experiments have indicated that our method not only achieves state-of-the-art results on several mainstream person Re-ID datasets, but also push the state-of-the-art performance to an exceptional level comparing to existing methods.

References

- [1] E. Ahmed, M. Jones, and T. K. Marks. An improved deep learning architecture for person re-identification. In *Proceedings of the IEEE Conference on Computer Vision and Pattern Recognition*, pages 3908–3916, 2015.
- [2] J. Almazan, B. Gajic, N. Murray, and D. Larlus. Re-id done right: towards good practices for person re-identification. *arXiv preprint arXiv:1801.05339*, 2018.
- [3] X. Bai, M. Yang, T. Huang, Z. Dou, R. Yu, and Y. Xu. Deep-person: Learning discriminative deep features for person re-identification. *arXiv preprint arXiv:1711.10658*, 2017.
- [4] X. Chang, T. M. Hospedales, and T. Xiang. Multi-level factorisation net for person re-identification. In *Proceedings of the IEEE conference on computer vision and pattern recognition*, 2018.
- [5] B. Chen, W. Deng, and J. Du. Noisy softmax: improving the generalization ability of dcnn via postponing the early softmax saturation. *arXiv preprint arXiv:1708.03769*, 2017.
- [6] W. Chen, X. Chen, J. Zhang, and K. Huang. Beyond triplet loss: a deep quadruplet network for person re-identification. In *Proceedings of the IEEE conference on computer vision and pattern recognition*, pages 403–412, 2017.
- [7] Y. Chen, X. Zhu, and S. Gong. Person re-identification by deep learning multi-scale representations. In *Proceedings of the IEEE International Conference on Computer Vision*, pages 2590–2600, 2017.
- [8] D. Cheng, Y. Gong, S. Zhou, J. Wang, and N. Zheng. Person re-identification by multi-channel parts-based cnn with improved triplet loss function. In *Proceedings of the IEEE Conference on Computer Vision and Pattern Recognition*, pages 1335–1344, 2016.
- [9] J. Deng, W. Dong, R. Socher, L.-J. Li, K. Li, and L. Fei-Fei. Imagenet: A large-scale hierarchical image database. In *Computer Vision and Pattern Recognition, 2009. CVPR 2009. IEEE Conference on*, pages 248–255. IEEE, 2009.
- [10] G. Ding, S. Khan, Z. Tang, and F. Porikli. Let features decide for themselves: Feature mask network for person re-identification. *arXiv preprint arXiv:1711.07155*, 2017.
- [11] P. Felzenszwalb, D. McAllester, and D. Ramanan. A discriminatively trained, multiscale, deformable part model. In *Computer Vision and Pattern Recognition, 2008. CVPR 2008. IEEE Conference on*, pages 1–8. IEEE, 2008.
- [12] Y. Guo and L. Zhang. One-shot face recognition by promoting underrepresented classes. *arXiv preprint arXiv:1707.05574*, 2017.
- [13] R. Hadsell, S. Chopra, and Y. LeCun. Dimensionality reduction by learning an invariant mapping. In *Computer vision and pattern recognition, 2006 IEEE computer society conference on*, volume 2, pages 1735–1742. IEEE, 2006.
- [14] K. He, X. Zhang, S. Ren, and J. Sun. Deep residual learning for image recognition. In *Proceedings of the IEEE conference on computer vision and pattern recognition*, pages 770–778, 2016.
- [15] A. Hermans, L. Beyer, and B. Leibe. In defense of the triplet loss for person re-identification. *arXiv preprint arXiv:1703.07737*, 2017.
- [16] E. Hoffer and N. Ailon. Deep metric learning using triplet network. In *International Workshop on Similarity-Based Pattern Recognition*, pages 84–92. Springer, 2015.
- [17] S. Ioffe and C. Szegedy. Batch normalization: Accelerating deep network training by reducing internal covariate shift. *arXiv preprint arXiv:1502.03167*, 2015.
- [18] D. P. Kingma and J. Ba. Adam: A method for stochastic optimization. *arXiv preprint arXiv:1412.6980*, 2014.
- [19] D. Li, X. Chen, Z. Zhang, and K. Huang. Learning deep context-aware features over body and latent parts for person re-identification. In *Proceedings of the IEEE Conference on Computer Vision and Pattern Recognition*, pages 384–393, 2017.
- [20] W. Li, R. Zhao, T. Xiao, and X. Wang. Deepreid: Deep filter pairing neural network for person re-identification. In *Proceedings of the IEEE Conference on Computer Vision and Pattern Recognition*, pages 152–159, 2014.
- [21] W. Li, X. Zhu, and S. Gong. Person re-identification by deep joint learning of multi-loss classification. *arXiv preprint arXiv:1705.04724*, 2017.
- [22] W. Li, X. Zhu, and S. Gong. Harmonious attention network for person re-identification. In *Proceedings of the IEEE conference on computer vision and pattern recognition*, 2018.
- [23] S. Liao, Y. Hu, X. Zhu, and S. Z. Li. Person re-identification by local maximal occurrence representation and metric learning. In *Proceedings of the IEEE Conference on Computer Vision and Pattern Recognition*, pages 2197–2206, 2015.
- [24] H. Liu, J. Feng, M. Qi, J. Jiang, and S. Yan. End-to-end comparative attention networks for person re-identification. *IEEE Transactions on Image Processing*, 26(7):3492–3506, 2017.
- [25] X. Liu, H. Zhao, M. Tian, L. Sheng, J. Shao, S. Yi, J. Yan, and X. Wang. Hydraplus-net: Attentive deep features for pedestrian analysis. In *Proceedings of the IEEE Conference on Computer Vision and Pattern Recognition*, pages 350–359, 2017.
- [26] X. Qian, Y. Fu, W. Wang, T. Xiang, Y. Wu, Y.-G. Jiang, and X. Xue. Pose-normalized image generation for person re-identification. *arXiv preprint arXiv:1712.02225*, 2017.
- [27] E. Ristani, F. Solera, R. Zou, R. Cucchiara, and C. Tomasi. Performance measures and a data set for multi-target, multi-camera tracking. In *European Conference on Computer Vision workshop on Benchmarking Multi-Target Tracking*, 2016.
- [28] M. S. Sarfraz, A. Schumann, A. Eberle, and R. Stiefelhagen. A pose-sensitive embedding for person re-identification with expanded cross neighborhood re-ranking. *arXiv preprint arXiv:1711.10378*, 2017.

- [29] F. Schroff, D. Kalenichenko, and J. Philbin. Facenet: A unified embedding for face recognition and clustering. In *Proceedings of the IEEE conference on computer vision and pattern recognition*, pages 815–823, 2015.
- [30] K. Sohn. Improved deep metric learning with multi-class n-pair loss objective. In *Advances in Neural Information Processing Systems*, pages 1857–1865, 2016.
- [31] H. O. Song, Y. Xiang, S. Jegelka, and S. Savarese. Deep metric learning via lifted structured feature embedding. In *Computer Vision and Pattern Recognition (CVPR), 2016 IEEE Conference on*, pages 4004–4012. IEEE, 2016.
- [32] C. Su, J. Li, S. Zhang, J. Xing, W. Gao, and Q. Tian. Pose-driven deep convolutional model for person re-identification. In *Proceedings of the IEEE International Conference on Computer Vision*, pages 3980–3989, 2017.
- [33] Y. Sun, L. Zheng, W. Deng, and S. Wang. Svdnet for pedestrian retrieval. In *Proceedings of the IEEE International Conference on Computer Vision*, pages 2590–2600, 2017.
- [34] Y. Sun, L. Zheng, Y. Yang, Q. Tian, and S. Wang. Beyond part models: Person retrieval with refined part pooling. *arXiv preprint arXiv:1711.09349*, 2017.
- [35] R. R. Viorio, M. Haloi, and G. Wang. Gated siamese convolutional neural network architecture for human re-identification. In *European Conference on Computer Vision*, pages 791–808. Springer, 2016.
- [36] Y. Wen, K. Zhang, Z. Li, and Y. Qiao. A discriminative feature learning approach for deep face recognition. In *European Conference on Computer Vision*, pages 499–515. Springer, 2016.
- [37] T. Xiao, H. Li, W. Ouyang, and X. Wang. Learning deep feature representations with domain guided dropout for person re-identification. In *Proceedings of the IEEE Conference on Computer Vision and Pattern Recognition*, pages 1249–1258, 2016.
- [38] H. Yao, S. Zhang, Y. Zhang, J. Li, and Q. Tian. Deep representation learning with part loss for person re-identification. *arXiv preprint arXiv:1707.00798*, 2017.
- [39] D. Yi, Z. Lei, S. Liao, and S. Z. Li. Deep metric learning for person re-identification. In *IEEE International Conference on Pattern Recognition*, pages 34–39, 2014.
- [40] X. Zhang, H. Luo, X. Fan, W. Xiang, Y. Sun, Q. Xiao, W. Jiang, C. Zhang, and J. Sun. Alignedreid: Surpassing human-level performance in person re-identification. *arXiv preprint arXiv:1711.08184*, 2017.
- [41] Y. Zhang, T. Xiang, T. M. Hospedales, and H. Lu. Deep mutual learning. *arXiv preprint arXiv:1706.00384*, 2017.
- [42] H. Zhao, M. Tian, S. Sun, J. Shao, J. Yan, S. Yi, X. Wang, and X. Tang. Spindle net: Person re-identification with human body region guided feature decomposition and fusion. In *Proceedings of the IEEE Conference on Computer Vision and Pattern Recognition*, pages 1077–1085, 2017.
- [43] L. Zhao, X. Li, J. Wang, and Y. Zhuang. Deeply-learned part-aligned representations for person re-identification. pages 3219–3228, 2017.
- [44] L. Zheng, L. Shen, L. Tian, S. Wang, J. Wang, and Q. Tian. Scalable person re-identification: A benchmark. In *Proceedings of the IEEE International Conference on Computer Vision*, 2015.
- [45] L. Zheng, Y. Yang, and A. G. Hauptmann. Person re-identification: Past, present and future. *arXiv preprint arXiv:1610.02984*, 2016.
- [46] Y. Zheng, D. K. Pal, and M. Savvides. Ring loss: Convex feature normalization for face recognition. In *Proceedings of the IEEE conference on computer vision and pattern recognition*, 2018.
- [47] Z. Zheng, L. Zheng, and Y. Yang. Pedestrian alignment network for large-scale person re-identification. *arXiv preprint arXiv:1707.00408*, 2017.
- [48] Z. Zheng, L. Zheng, and Y. Yang. Unlabeled samples generated by gan improve the person re-identification baseline in vitro. In *Proceedings of the IEEE International Conference on Computer Vision*, 2017.
- [49] Z. Zhong, L. Zheng, D. Cao, and S. Li. Re-ranking person re-identification with k-reciprocal encoding. In *Computer Vision and Pattern Recognition (CVPR), 2017 IEEE Conference on*, pages 3652–3661. IEEE, 2017.